Published in final edited form as:
Mol Cell Neurosci. 2007 May ; 35(1): 161–170.

Carbonic anhydrase related protein 8 mutation results in aberrant synaptic morphology and excitatory synaptic function in the cerebellum

Michiru Hirasawa[3,4], **Xinjie Xu**[1], **Robert B. Trask**[3], **Terry P. Maddatu**[2], **Britt A Johnson**[1], **Jürgen K. Naggert**[2], **Patsy M. Nishina**[2], and **Akihiro Ikeda**[1,4]

1 *Department of Medical Genetics, University of Wisconsin-Madison, Madison, WI 53706, USA*

2 *The Jackson Laboratory, Bar Harbor, ME 04609, USA*

3 *Division of Basic Medical Sciences, Memorial University of Newfoundland, St. John's, Newfoundland A1B 3V6, Canada*

Abstract

Carbonic anhydrase related protein 8 (*Car8*) is known to be abundantly expressed in Purkinje cells (PCs), and its genetic mutation causes a motor coordination defect. To determine the underlying mechanism, we analyzed the mouse cerebellum carrying a *Car8* mutation. Electrophysiological analysis showed that spontaneous excitatory transmission was largely diminished while paired pulse ratio at parallel fiber-PC synapses was comparable to wild-type, suggesting functional synapses have normal release probability but the number of functional synapses may be lower in mutants. Light microscopic study revealed an abnormal extension of climbing fibers to the distal PC dendrites. At ultrastructural level, we found numerous PC spines not forming synapses primarily in distal dendrites and occasionally multiple spines contacting a single varicosity. These abnormalities of parallel fiber-PC synapses may underlie the functional defect in excitatory transmission. Thus, *Car8* plays a critical role in synaptogenesis and/or maintenance of proper synaptic morphology and function in the cerebellum.

Introduction

Cerebellum is the primary motor coordination center that receives various sensory inputs and generates motor-related outputs (Apps & Garwicz, 2005). Two main afferent inputs to the cerebellum are mossy fibers originating from the brain stem and spinal cord, and climbing fibers (CFs) from the inferior olivary nucleus. Mossy fibers innervate granule cells in the cerebellum, which in turn excite Purkinje cells (PCs) through parallel fibers (PFs), while CFs directly innervate PCs. PCs, then, provide the sole output of the cerebellar cortex. Thus,

[4]Address correspondence to: Akihiro Ikeda, Ph.D., Department of Medical Genetics, University of Wisconsin-Madison, 445 Henry Mall, Room 5322 Genetics/Biotech, Madison, WI 53706, Office Tel: +1-(608)262-5477, Lab Tel: +1-(608)262-5991, Fax: +1-(608)262-2976, email: aikeda@wisc.edu.
Michiru Hirasawa, Ph.D., Division of Basic Medical Sciences, Faculty of Medicine, Memorial University of Newfoundland, 300 Prince Philip Drive, St. John's, Newfoundland A1B 3V6, Canada
Tel: 709-777-6727, Fax: 709-777-7010, e-mail: michiru@mun.ca

appropriate wiring and synaptic activity converging onto PCs are a prerequisite for proper cerebellar function.

Carbonic anhydrase related protein 8 (CAR8) is a molecule that is highly expressed in the cerebellum, in particular PCs (Kato, 1990;Nogradi *et al*., 1997; Hirota *et al*., 2003;Jiao *et al*., 2005) while lower levels of expression has been observed in cerebellar nuclei and brainstem (Jiao *et al*., 2005). CAR8 belongs to a large family of carbonic anhydrases that are important for many biological functions including respiration, calcification, acid-base balance, bone resorption and the formation of aqueous humor (Dodgson *et al*. 1991). However, unlike other family members of carbonic anhydrases, CAR8 does not have the catalytic carbonic anhydrase activity, as it lacks the necessary catalytic zinc coordinating residues (Kato, 1990;Sjoblom *et al*., 1996).

Evidence for CAR8 playing a critical role in motor coordination came from waddles mice (*wdl*) that carry a spontaneous mutation in the *Car8* gene (http://www.jax.org/mmr/waddler.html). These mice display a characteristic wobbly side-to-side ataxic movement from an early postnatal age (Jiao *et al*., 2005), however, the morphology of the cerebellum appeared normal by confocal microscopy (Jiao *et al*., 2005). Thus, the mechanism underlying the behavioral defect remained unknown. In this study, we took advantage of the *Car8* mutant mice to investigate the functional and structural consequences of the functional deletion of this protein. Our results demonstrate that *Car8* is necessary for the normal development and/or maintenance of the morphology and function of excitatory synapses in the cerebellum.

Results

Origin of *Car8* mutant mice

A sponteneous recessive mutation Rigoletto (*rig*), characterized by wobbly side-to-side ataxic movements was isolated from an experimental C57BLKS/J-*fat*/+ colony. Rotarod analysis showed that *rig* mice have motor disability (result not shown). Morphological analysis at the light microscopic level did not reveal any gross abnormalities in the cerebellum of *rig* mice (Fig. 1A–D). By immunostaining cerebellar sections using anti-calbindin, we further confirmed the existence of dendritic spines in PCs of *rig* mice and examined their morphology at a higher magnification (×100) using confocal microscopy (Fig. 1E and F). This analysis did not reveal any differences in the shape and size of the dendritic spine (area occupied by each spine head: 0.162 ± 0.010 μm^2 in wild-type [n=4] vs 0.157 ± 0.010 μm^2 in *rig* [n=4] mice; p=0.732).

Our genetic mapping using 1266 F2 animals from mating (*rig* × CAST/EiJ) F1 mice demonstrated that the recessive *rig* mutation was mapped to the region flanked by markers D4Mit50 and D4Mit264 on chromosome 4, which included the *Car8* gene. Subsequent sequence analysis showed that the *Car8* gene in *rig* mice contains a 19 bp deletion, identical to the mutation in *wdl* mice (Jiao *et al*., 2005). Based on the very similar phenotypes between *rig* and *wdl* mice (Jiao *et al*., 2005) and the fact that the *Car8* gene carried this uncommon sequence change within the *rig* minimal region, (Jiao *et al*., 2005) in *rig* mice, we concluded that 1) *rig* phenotypes are caused by the 19bp deletion in the *Car8* gene and that 2) *rig* and *wdl* mutations are identical and highly likely originate from a spontaneous mutation that occurred in the C57BLKS/J colony at The Jackson Laboratory. Therefore, we will refer to the mutant allele in *rig* mutants as $Car8^{wdl}$ hereafter in this manuscript.

Electrophysiological study

To examine whether any defect in excitatory synaptic function can be observed at the cellular level, we performed whole cell patch clamp recordings from PCs. The basal frequency of spontaneous excitatory postsynaptic currents (EPSCs) in wild-type was 7.5 ± 0.8 Hz (n=8), which is in the similar range as previous reports (Chen & Regehr, 1997;Takahashi & Linden, 2000). Absence or presence of tetrodotoxin (TTX) did not significantly change the frequency of spontaneous EPSCs (data not shown), indicating that the majority of spontaneous glutamate release onto PCs was action potential-independent miniature EPSCs (mEPSC) in our preparation. Thus, data obtained with or without TTX were pooled. In contrast to wild-type, the frequency of mEPSC was much fewer in *Car8*^{wdl} mice (2.0 ± 0.6 Hz, n=7; $p<0.05$ vs. wild-type; Fig. 2A1, A2), while the amplitude of mEPSC was similar between wild-type and *Car8*^{wdl} mice (17.8 ± 2.4 Hz vs. 16.8 ± 1.0 Hz, $p>0.05$) (Fig. 2A3). By contrast, the paired pulse ratio at PF-PC synapse was not statistically different (wild-type 1.66 ± 0.1, n=5 vs. *Car8*^{wdl} 1.63 ± 0.1 Hz, n=4; $p>0.05$; Fig. 2B1, B2), suggesting that the release probability of glutamate at the functional synapses formed between PF and PC is normal. Therefore, lower frequency of excitatory transmission may indicate a lower number of functional synaptic connections.

Parallel fiber and climbing fiber innervation

To determine whether there is any apparent difference in the innervation of PF and CF to PC, immunofluorescence staining was performed for the vesicular glutamate transporter (VGLUT) 1 and VGLUT2 as markers for PF and CF terminals, respectively (Fremeau *et al*. 2001, Ichikawa *et al.* 2002, Miyazaki *et al.* 2003). The density of VGLUT2-positive CF terminals in the molecular layer of *Car8*^{wdl} mice was higher than that in wild-type mice (0.0076 ± 0.0010 puncta per μm^2 in wild-type [n=5] mice vs 0.0147 ± 0.0031 puncta per μm^2 in *Car8*^{wdl} [n=5]; p=0.04; Fig. 3A–D). In addition, VGLUT2-positive puncta were observed in wider area in the *Car8*^{wdl} cerebellum, penetrating 88.8 ± 1.5% (n=6) of the molecular layer thickness measured from the boundary juxtaposing the granule layer, while it was significantly less (82.0 ± 1.8%, n=6, P=0.008) in the wild-type cerebellum. CF terminals were mainly associated with primary dendritic shafts in wild-type cerebellum (Fig. 3C), while they were also found in association with the distal spiny branchlets in the *Car8*^{wdl} cerebellum (Fig. 3D). In contrast, there was no apparent difference in the distribution of VGLUT1-positive PF terminals which was found throughout the molecular layer in both wild type and *Car8*^{wdl} mice (Fig. 3E, F). These observations, however, do not explain the reduction in excitatory transmission to PCs in *Car8*^{wdl} mice. Thus, there may be other synaptic abnormalities that cannot be detected by light microscopy.

Ultrastructural abnormalities of PF-PC synapses in the Car8^{wdl} cerebellum

In order to investigate whether the *Car8*^{wdl} cerebellum shows morphological aberration that can be detected only at the electron microscopic level, we examined its ultrastructural morphology and compared to that of wild-type cerebellum. The areal density of PC dendritic spines was similar between wild-type and *Car8*^{wdl} mice (Fig. 4C; p=0.3939). PF varicosities were observed in both wild-type and mutant animals as small presynaptic axon enlargements that contain synaptic vesicles and mitochondria, forming asymmetric synapses with dendritic spines of PCs. In addition, the mutants had numerous free spines that do not form synapses (Fig. 4A, B). A significantly larger number of free spines were found in mutant mice (30.5%; n=6; total 3598 spines examined) compared with wild-type mice (0.9%; n=6; total 3559 spines examined). We also examined the distribution of free spines within the molecular layer. The number of free spines were counted in the region adjacent to the distal border of the molecular layer (distal) where synaptic inputs originate almost exclusively from PF, and in the region adjacent to the PC soma (peri-PC soma) where both PF and CF terminals exist. PF terminals

still account for the majority of excitatory input in the peri-PC soma area where they innervate spines originating from distal spiny branchlets, whereas CF terminals innervate proximal dendrites. Free spines were observed in both regions with greater number in the distal molecular layer (Fig. 4D). These free spines contained postsynaptic density (PSD)-like condensations and endoplasmic reticulum, and often appeared in clusters (Fig. 4A, B). Examination of serial sections confirmed that in both wild-type and *Car8*^{wdl} mice, the region of dendritic spines contacted by presynaptic terminals always contained PSD (data not shown), whereas free spines had PSD-like condensations but did not contact any presynaptic counterparts (Fig. 4E–L).

Other mutant mice known to have free spines, such as ionotropic glutamate receptor delta 2 (*Grid2*) and cerebellin 1 precursor protein (*Cbln1*) deficient mice, also exhibit mismatching between PSD and the presynaptic active zone (Takeuchi *et al*. 2005, Hirai *et al.* 2005). Therefore, we examined if this is also apparent in *Car8*^{wdl} mice. Electron microscopic images were analyzed for potential mismatching of PSD and the active zone at the synapse characterized by separation of their edges by more than 100nm (definition used in Takeuchi *et al*. 2005 & Hirai *et al*. 2005). Among 485 synapses examined in *Car8*^{wdl} mice, there were no synapses that fitted this criterion.

We also observed increased number of multiple synaptic varicosities (2–4 dendritic spines contacting one varicosity) in the mutants. As summarized in Fig. 5G, the percentage of the multiple synapses (pre vs post being 1:2 and higher) was significantly higher in *Car8*^{wdl} mice (2.40% in wild-type [n=6] vs 8.95% in *Car8*^{wdl} [n=6]; $P<0.005$). 1:3 or 1:4 multiple synaptic varicosities comprised 1.35% of the total number of synapses in mutant mice (Fig. 5H) while these were never found in wild-type mice. The size of varicosities comprising these synapses was larger than those in 1:1 synapses. Nonetheless, synaptic vesicles were clustered towards each PSD just as in 1:1 or 1:2 synapses (Fig. 5A–F). Regardless of its presynaptic counterpart, the structure of each spine appeared to be normal with respect to the existence of PSD and endoplasmic reticulum membrane in *Car8*^{wdl} mice (Fig. 5).

Discussion

The present study demonstrates that the mutation in the *Car8* gene causes structural as well as functional abnormalities of excitatory synapses onto PCs in the cerebellum. Since the 19 bp deletion in the *Car8* gene is likely to be a loss of function mutation (Jiao *et al*., 2005), our results indicate that *Car8* is critical for proper development and/or maintenance of excitatory PC synapses.

Our electrophysiological analysis revealed that the *Car8* mutation leads to a significant reduction of the rate of spontaneous excitatory neurotransmission onto PCs. This may be due to less number of excitatory synapses and/or lower release probability, i.e. lower rate of transmitter release at each synapse. Excitatory synaptic inputs to PCs are supplied from PFs and CFs. According to our light microscopic study, CFs innervate more densely and extend further distally in the molecular layer in the *Car8*^{wdl} cerebellum. In contrast, electron microscopic study suggests that significant number of PC dendritic spines is not forming synapses, particularly in distal dendrites where PFs normally form synapses. Therefore, it is most likely that the diminution in spontaneous excitatory transmission is due to reduced PF innervation to PCs. However, to fully account for the large reduction in spontaneous excitatory transmission (approx 73.2% reduction in mEPSC frequency vs. 30.5% free spines), the rate of transmission at existing functional synapses and/or the number of active synapses must also be limited in *Car8*^{wdl} mice. The paired pulse ratio at PF-PC synapses showing no differences between the two groups of animals support the latter possibility. In other words, some of the

spines that form morphologically intact synapses with PFs may not be functionally active, whereas the functional synapses have normal release probability.

One of the most prominent morphological change caused by the *Car8* gene mutation was impaired formation and/or maintenance of synapses, generating numerous free dendritic spines that contain PSD-like condensations but lack presynaptic counterparts. These free spines of *Car8*^{wdl} mutants may represent stable spines, because it has been shown that PSD-95 clustering at filopodia is associated with stabilization of spines and synapse formation (Prange & Murphy, 2001). The total numbers of spines in a unit area in wild-type and *Car8*^{wdl} animals were similar, suggesting that the spine formation/maintenance *per se* is unaffected in the mutants.

Free spines were abundantly observed in the distal region of the molecular layer (Fig. 4D), where synaptic inputs originate almost exclusively from PF rather than CF, even in *Car8*^{wdl} mice (Fig. 3D, F). Therefore, it appears that PF-PC interactions are significantly inhibited by the *Car8*^{wdl} mutation, concurrently with the extensive CF innervation. It has been proposed that the proper innervation of PFs and CFs along the PC dendrites is achieved through the balancing of two distinct mechanisms that intensely compete with each other: one that stabilizes PF synapses and restricts CF innervation to the proximal dendrites, and one that strengthens CF synapses and restricts PF innervation distally (Ichikawa *et al*., 2002;Miyazaki *et al*., 2004). With these 2 mechanisms properly balanced, PFs innervate the distal dendrites while CFs innervate the proximal dendrites. Our result indicates that CAR8 plays a role in this mechanism by suppressing CF and/or promoting PF innervation.

Another morphological abnormality in *Car8*^{wdl} mice, although less common, was multiple synaptic varicosities marked by more than 2 dendritic spines contacting a single varicosity. The morphology of these varicosities is not consistent with that of CF terminals which typically have densely packed synaptic vesicles and darker cytoplasm (Ichikawa *et al*., 2002;Rhyu *et al*., 1999a;Xu-Friedman *et al*., 2001). Therefore, these multiple synaptic varicosities are most likely formed between PF and PC. The highest number of spines we observed comprising a multiple synaptic varicosity was 4. This could be an underestimate since 3D reconstruction of complete varicosities may reveal higher number of spines per varicosity. Nonetheless, we never observed a multiple synaptic varicosity with more than two spines in wild-type animals, indicating that those having more than two spines are not normal. 1:2 multiple spines can be observed in physiological conditions as an intermediate form of synaptogenesis induced by activity dependent long term potentiation (Nikonenko *et al*., 2002) and motor learning (Kim *et al*., 2002). In *Car8*^{wdl} mutants, varicosities with 3 or 4 spines tend to be larger, which may indicate that the varicosities did not properly split to generate new synapses.

Mice deficient for *Grid2* and *Cbln1* are mouse models known to be ataxic and have abnormal synaptic morphology in the cerebellum similar to *Car8*^{wdl} mutants (Kashiwabuchi *et al*. 1995; Kurihara *et al*., 1997; Hirai *et al*., 2005). GRID2 is a glutamate receptor subunit predominantly expressed in PCs (Araki *et al*., 1993;Lomeli *et al*., 1993) at postsynaptic dendritic sites apposing PF terminals (Landsend *et al*., 1997;Mayat *et al*., 1995;Takayama *et al*., 1995). CBLN1 is a cerebellum specific protein structurally related to C1q and tumor necrosis factor family (Kishore *et al*. 2004) that is expressed and secreted by cerebellar granule cells that give rise to PF (Hirai *et al*. 2005). Similar to *Car8*^{wdl} mutants, extension of CF territory has been found in mice deficient for *Grid2* (Ichikawa *et al*., 2002) and *Cbln1* (Hirai *et al*., 2005), suggesting that *Grid2*, *Cbln1* and *Car8* fuel the competition to be advantageous to PFs. The occurrence of free spines without a change in the total number of spines is also seen in mice deficient for *Grid2* (Kurihara *et al*., 1997) and *Cbln1* (Hirai *et al*., 2005). Based on the phenotypic similarities between the three mutant mice, we speculate that CAR8, GRID2 and CBLN1 work in concert for the formation and/or maintenance of PF synaptic contacts rather than spine formation. However, mismatched synapses, a feature seen in *Grid2* and *Cbln1*

mutants (Takeuchi *et al*. 2005;Hirai *et al*., 2005), were not found in *Car8*^{wdl} mutants. This may be an indication that formation of synaptic contacts and proper arrangement of PSD and active zone are differentially regulated. Another mouse model that displays ataxia and aberrant synaptic morphology is spontaneous or genetargeted mutant for *Cacna1a* (Jun *et al.* 1999; Miyazaki *et al*., 2004). CACNA1A is a P/Q type voltage-dependent calcium channel subunit (alpha 1A) expressed in cell bodies, dendrites and presynaptic terminals of neurons throughout the brain (Westenbroek *et al.* 1995). Multiple synaptic varicosity observed in *Car8*^{wdl} mice is a phenotype shared by these mutants (Rhyu *et al*., 1999a;Rhyu *et al*., 1999b; Miyazaki *et al*., 2004). Importantly, these abnormal synaptic units in *Cacna1a* mutants were observed before the onset of behavioral phenotypes, indicating that behavioral symptoms were not the cause of the morphological abnormality. A mutation in the *Cacna1a* gene also results in the expansion of PF territories (Miyazaki *et al*., 2004), in contrast to *Car8* mutation leading to extended CF territory. Taken together, the characteristics of *Car8*^{wdl} mutation, namely extension of CF territory, free spines and multiple synaptic varicosities, partially overlap with a number of mutants known to have synaptic defect in the cerebellum. However, none of them completely duplicates the phenotype of *Car8*^{wdl} mutants.

CAR8 was recently identified as a binding protein for the IP3 receptor type 1 which is most abundantly expressed in the PC of the cerebellum (Hirota *et al*., 2003). Binding of CAR8 to IP3 receptors reduces the affinity of the receptor to IP3 (Jiao *et al*., 2005). It is possible that *Car8* mutation disinhibits the interaction between IP3 and IP3 receptor, allowing extra calcium to be released from IP3-sensitive stores, resulting in the phenotype of *Car8*^{wdl} mice. In support of this possibility, relatively high levels of calcium in PC dendrites/spines caused by CF activation has been suggested to inhibit PF territory expansion (Bravin *et al*., 1999;Sotelo *et al*., 1975). On the other hand, elimination of CF or inactivation of CF-PC synapse with TTX, which inhibits large calcium transients in PC dendrites through voltage-gated calcium channels and IP3 signaling (Knopfel *et al*., 1991;Konnerth *et al*., 1992;Miyakawa *et al*., 1992;Okubo *et al*., 2001), results in extension of PF innervation to the proximal dendrites (Bravin *et al*., 1999;Sotelo *et al*., 1975). It is conceivable that CAR8 plays a role in fine-tuning of the intracellular calcium level in the PC dendrites to optimize PF innervation. Alternatively, we cannot rule out the possibility that the CAR8 function may involve yet unknown mechanisms independent of IP3 receptors which are essential for proper synaptic formation and/or maintenance in the cerebellum.

In conclusion, the mutation in the *Car8* gene leads to morphological and functional abnormalities of synapses onto PCs, which likely underlie the motor coordination defect in *Car8*^{wdl} mutant mice. Our data highlights the importance of this molecule in the development and/or maintenance of the proper morphology and function of PC synapses. Moreover, based on our findings and the possible role CAR8 has in IP3 and intracellular calcium signaling (Hirota *et al*., 2003), *Car8*^{wdl} animals may offer an interesting model by which intracellular calcium dependent processes in the cerebellum can be investigated.

Experimental methods

Animals

All experiments were performed in accordance with the National Institute of Health Guide for the Care and Use of Laboratory Animals and the Canadian Council on Animal Care guidelines, and were approved by the University of Wisconsin-Madison, The Jackson Laboratory and Memorial University of Newfoundland Animal Care and Use Committees.

Rigoletto (*rig*) mice (C57BLKS/J-*rig/rig*) were isolated and maintained in our experimental colony at The Jackson Laboratory. Age matched wild-type control C57BLKS/J (BKS), C57BL/

6J or 129S1/SvImJ mice, and CAST/EiJ (CAST) mice for genetic mapping were obtained from The Jackson Laboratory.

To map the *rig* gene, we performed a whole genome wide scan using F2 animals from mating (*rig* x CAST) F1 mice. We initially used 42 microsatellite markers, which distinguish BKS alleles from CAST alleles across the whole genome. All F2 animals were phenotyped by observing their ataxic locomotion. Once the chromosomal locus on chromosome 4 for the *rig* mutation was identified, additional F2 mice were collected and additional markers were used to further narrow the genetic region.

Immunohistochemistry

Wild-type and *Car8* mutant mice were deeply anesthetized with mixture of ketamine and xylazine and perfused with 4% paraformaldehyde (PFA). The heads were immersed in 4% PFA overnight at 4°C, and the brain was dissected out. For paraffin sections, the brain was dehydrated in a graded ethanol series, cleared in xylene, and embedded in paraffin. Sections were cut at 6 μm, mounted on slides pretreated with Vectabond (Vector Laboratories, Burlingame, CA). For cryostat sections, the brain was cryoprotected at 4°C in a graded series of sucrose after dissection. Brains were embedded in optimal temperature cutting compound (OCT) and sectioned at 12μm thickness.

For immunohistochemistry, sections were blocked with 2% donkey serum and were incubated overnight with the primary antibody against Calbindin-D (Swant, Bellinzona, Switzerland), IP3 receptor type 1 (Affinity BioReagents; Golden, CO), VGLUT1 (Synaptic Systems, Germany) or VGLUT2 (Synaptic Systems, Germany). Sections were rinsed in PBS, and incubated with a 1:200 diluted Alexa 488 conjugated secondary antibody (Invitrogen, Carlsbad, CA) in block solution for 45 minutes at room temperature. Control slides were prepared by omitting the primary antibody (data not shown). All sections were imaged on an Eclipse E600 microscope (Nikon, Tokyo, Japan) using a SPOT camera (Spot Diagnostics; Sterling Heights, MI) or a Zeiss Nipkow-disc based confocal microscope with a mercury lamp (Axiovert; Zeiss, Oberkochen, Germany) equipped with a CCD camera (Zeiss Axiocam ER; Zeiss, Oberkochen, Germany). For comparing the size and shape of Purkinje cell dendritic spines, images collected from sections stained with anti Calbindin-D antibody were used. The positively stained area occupied by each spine head was measured using NIH Image software.

Electrophysiological recording

Wild-type and *Car8* mutant mice (8 weeks to 5 months old) were decapitated under deep halothane anesthesia, and the brain was removed to generate 200μm transverse cerebellar slices at 0°C in a buffer solution (in mM): NaCl (87), KCl (2.5), NaH_2PO_4 (1.25), $MgCl_2$ (7), $CaCl_2$ (0.5) $NaHCO_3$ (25), glucose (25), sucrose (20). Slices were incubated at 32–34°C for an hour and then at room temperature until recording in artificial cerebrospinal fluid (ACSF) (in mM): NaCl (126), KCl (2.5), NaH_2PO_4 (1.2), $MgCl_2$ (1.2), $CaCl_2$ (2.4) $NaHCO_3$ (18), glucose (11). Both solutions were continuously bubbled with O_2 (95%) and CO_2 (5%).

Cerebellar slices were placed in the recording chamber and perfused with ACSF (33–34°C). PCs were visualized by a DIC-IR microscope and identified based on their localization and shape. Nystatin-perforated patch whole cell recording (series/access resistance: 10–30M was performed with electrodes having a tip resistance of 3–7ω˜ Internal recording solution (pH 7.3) contained (in mM): K-gluconate (120), $MgCl_2$ (5), EGTA (10), HEPES (40). Nystatin was dissolved in DMSO with Pluronic F127 and added to the internal solution (final concentration: 450μg/ml). Multiclamp 700B amplifier (Axon Instruments) was used to monitor synaptic currents in voltage clamp mode (holding potential=−60mV) or resting membrane potential and spontaneous firing activity in current clamp mode. Signals were filtered at 1 kHz, digitized at

5–10 kHz and stored for off-line analysis using pClamp 9 software (Axon Instruments). Input resistance and series/access resistance were monitored regularly throughout each experiment. To isolate excitatory postsynaptic currents (EPSCs), picrotoxin 50μM was added to block GABAA receptor mediated currents.

For paired pulse protocol, synaptic currents were evoked with a glass pipette filled with ACSF placed in the molecular layer to directly activate parallel fiber activity. Stimulus intensities of 50–70% maximum evoked EPSC amplitude were used. Every 15 sec, a pair of afferent stimulation with 50 ms interval was given. The paired pulse ratio was determined by dividing the amplitude of the second EPSC by the first EPSC. Spontaneous or miniature EPSCs (mEPSCs) were recorded in the presence of tetrodotoxin (TTX: 1mM), analysed using MiniAnalysis software (Synaptosoft Inc. GA) and detected if the amplitude was larger than 4–5 times the RMS noise. Cumulative plots for interevent interval and amplitude were obtained as relative frequencies for each cell and pooled according to their genetic phenotype. Kolmogorov-Smirnov test and Student t-test were used, $p<0.05$ was deemed significant.

Electron microscopy

Wild-type (C57BL/6J, 129S1/SvImJ or their mixture) and *Car8* mutant mice that are developmentally mature (5weeks to 10 months old) (McKay & Turner, 2005) were anesthetized with ketamine/xylazine and perfused with 2% PFA and 2.5% glutaraldehyde in 0.1M phosphate buffer for 11 min. Cerebella were removed from the head and immersion fixed for 30 min. Then, cerebella were sagitally sectioned at 100μm intervals with vibratome. Sections of cerebella were osmicated (1% osmium tetroxide) for 1 hr and washed in 0.1M phosphate buffer, dehydrated through an ascending series of ethanol and propylene oxide and embedded in Epon. Ultra-thin sections (70nm) were cut and stained with uranyl acetate and lead citrate. Sections were imaged on a Philips CM120 Scanning Transmission Electron Microscope. For examining the distribution of dendritic spines, spines were counted in areas that are adjacent to the distal border of the molecular layer (distal) and to the Pukinje cell soma (peri-PC soma). Statistical comparison was performed using Student's t-test.

Acknowledgements

The original spontaneous mutant was first identified, heritability tested, and named rigoletto by Dr. Konrad Noben-Trauth. The authors thank Satoshi Kinoshita for generating frozen sections, Lance Rodenkirch, Michael Hendrickson, Benjamin August, Randall Massey and Caroline Smith for the technical support, The W.M. Keck Laboratory for Biological Imaging for the use of the confocal microscope, the University of Wisconsin Medical School Electron Microscope Facility for use of the facility equipment and Dr. Sakae Ikeda for critical reading of the manuscript. This study was supported by grants from National Institutes of Health (NIH). Support for BAJ was provided by the Predoctoral Training Program in Genetics, 5 T32 GM07133. MH is a Canadian Institutes of Health Research New Investigator.

References

Apps R, Garwicz M. Anatomical and physiological foundations of cerebellar information processing. Nat Rev Neurosci 2005;6:297–311. [PubMed: 15803161]

Araki K, Meguro H, Kushiya E, Takayama C, Inoue Y, Mishina M. Selective expression of the glutamate receptor channel delta 2 subunit in cerebellar Purkinje cells. Biochem Biophys Res Commun 1993;197:1267–1276. [PubMed: 7506541]

Bliss TV, Collingridge GL. A synaptic model of memory: long-term potentiation in the hippocampus. Nature 1993;361:31–39. [PubMed: 8421494]

Bravin M, Morando L, Vercelli A, Rossi F, Strata P. Control of spine formation by electrical activity in the adult rat cerebellum. Proc Natl Acad Sci U S A 1999;96:1704–1709. [PubMed: 9990088]

Chen C, Regehr WG. The mechanism of cAMP-mediated enhancement at a cerebellar synapse. J Neurosci 1997;17(22):8687–8694. [PubMed: 9348337]

Dodgson, SJ.; Tashian, RE.; Gross, G.; Carter, ND. The Carbonic Anhydrases: Cellular Physiology and Molecular Genetics. Springer, New York: Plenum; 1991.

Fitzsimonds RM, Poo MM. Retrograde signaling in the development and modification of synapses. Physiol Rev 1998;78:143–170. [PubMed: 9457171]

Fremeau RT Jr, Troyer MD, Pahner I, Nygaard GO, Tran CH, Reimer RJ, Bellocchio EE, Fortin D, Storm-Mathisen J, Edwards RH. The expression of vesicular glutamate transporters defines two classes of excitatory synapse. Neuron 2001;31(2):247–260. [PubMed: 11502256]

Hirai H, Pang Z, Bao D, Miyazaki T, Li L, Miura E, Parris J, Rong Y, Watanabe M, Yuzaki M, Morgan JI. Cbln1 is essential for synaptic integrity and plasticity in the cerebellum. Nat Neurosci 2005;8(11): 1534–1541. [PubMed: 16234806]

Hirota J, Ando H, Hamada K, Mikoshiba K. Carbonic anhydrase-related protein is a novel binding protein for inositol 1,4,5-trisphosphate receptor type 1. Biochem J 2003;372:435–441. [PubMed: 12611586]

Ichikawa R, Miyazaki T, Kano M, Hashikawa T, Tatsumi H, Sakimura K, Mishina M, Inoue Y, Watanabe M. Distal extension of climbing fiber territory and multiple innervation caused by aberrant wiring to adjacent spiny branchlets in cerebellar Purkinje cells lacking glutamate receptor delta 2. J Neurosci 2002;22:8487–8503. [PubMed: 12351723]

Jiao Y, Yan J, Zhao Y, Donahue LR, Beamer WG, Li X, Roe BA, Ledoux MS, Gu W. Carbonic anhydrase-related protein VIII deficiency is associated with a distinctive lifelong gait disorder in waddles mice. Genetics 2005;171:1239–1246. [PubMed: 16118194]

Jun K, Piedras-Renteria ES, Smith SM, Wheeler DB, Lee SB, Lee TG, Chin H, Adams ME, Scheller RH, Tsien RW, Shin HS. Ablation of P/Q-type Ca(2+) channel currents, altered synaptic transmission, and progressive ataxia in mice lacking the alpha(1A)-subunit. Proc Natl Acad Sci U S A 1999;96:15245–15250. [PubMed: 10611370]

Kalinovsky A, Scheiffele P. Transcriptional control of synaptic differentiation by retrograde signals. Curr Opin Neurobiol 2004;14:272–279. [PubMed: 15194106]

Kashiwabuchi N, Ikeda K, Araki K, Hirano T, Shibuki K, Takayama C, Inoue Y, Kutsuwada T, Yagi T, Kang Y, Aizawa S, Mishina M. Impairment of motor coordination, Purkinje cell synapse formation, and cerebellar long-term depression in GluR delta 2 mutant mice. Cell 1995;81:245–252. [PubMed: 7736576]

Kato K. Sequence of a novel carbonic anhydrase-related polypeptide and its exclusive presence in Purkinje cells. FEBS Lett 1990;271:137–140. [PubMed: 2121526]

Kim HT, Kim IH, Lee KJ, Lee JR, Park SK, Chun YH, Kim H, Rhyu IJ. Specific plasticity of parallel fiber/Purkinje cell spine synapses by motor skill learning. Neuroreport 2002;13:1607–1610. [PubMed: 12352611]

Kishore U, Gaboriaud C, Waters P, Shrive AK, Greenhough TJ, Reid KB, Sim RB, Arlaud GJ. C1q and tumor necrosis factor superfamily: modularity and versatility. Trends Immunol 2004;25(10):4551–561.

Knopfel T, Vranesic I, Staub C, Gahwiler BH. Climbing Fibre Responses in Olivo-cerebellar Slice Cultures. II. Dynamics of Cytosolic Calcium in Purkinje Cells. Eur J Neurosci 1991;3:343–348. [PubMed: 12106192]

Konnerth A, Dreessen J, Augustine GJ. Brief dendritic calcium signals initiate long-lasting synaptic depression in cerebellar Purkinje cells. Proc Natl Acad Sci U S A 1992;89:7051–7055. [PubMed: 1323125]

Kurihara H, Hashimoto K, Kano M, Takayama C, Sakimura K, Mishina M, Inoue Y, Watanabe M. Impaired parallel fiber-->Purkinje cell synapse stabilization during cerebellar development of mutant mice lacking the glutamate receptor delta2 subunit. J Neurosci 1997;17:9613–9623. [PubMed: 9391016]

Landsend AS, Amiry-Moghaddam M, Matsubara A, Bergersen L, Usami S, Wenthold RJ, Ottersen OP. Differential localization of delta glutamate receptors in the rat cerebellum: coexpression with AMPA receptors in parallel fiber-spine synapses and absence from climbing fiber-spine synapses. J Neurosci 1997;17:834–842. [PubMed: 8987804]

Lomeli H, Sprengel R, Laurie DJ, Kohr G, Herb A, Seeburg PH, Wisden W. The rat delta-1 and delta-2 subunits extend the excitatory amino acid receptor family. FEBS Lett 1993;315:318–322. [PubMed: 8422924]

Maejima T, Hashimoto K, Yoshida T, Aiba A, Kano M. Presynaptic inhibition caused by retrograde signal from metabotropic glutamate to cannabinoid receptors. Neuron 2001;31(3):463–475. [PubMed: 11516402]

Maejima T, Oka S, Hashimotodani Y, Ohno-Shosaku T, Aiba A, Wu D, Waku K, Sugiura T, Kano M. Synaptically driven endocannabinoid release requires Ca2+-assisted metabotropic glutamate receptor subtype 1 to phospholipase Cbeta4 signaling cascade in the cerebellum. J Neurosci 2005;25 (29):6826–6835. [PubMed: 16033892]

Mayat E, Petralia RS, Wang YX, Wenthold RJ. Immunoprecipitation, immunoblotting, and immunocytochemistry studies suggest that glutamate receptor delta subunits form novel postsynaptic receptor complexes. J Neurosci 1995;15:2533–2546. [PubMed: 7891187]

McKay BE, Turner RW. Physiological and morphological development of the rat cerebellar Purkinje cell. J Physiology (Lond) 2005;567(Pt 3):829–850.

Miyakawa H, Lev-Ram V, Lasser-Ross N, Ross WN. Calcium transients evoked by climbing fiber and parallel fiber synaptic inputs in guinea pig cerebellar Purkinje neurons. J Neurophysiol 1992;68:1178–1189. [PubMed: 1359027]

Miyazaki T, Fukaya M, Shimizu H, Watanabe M. Subtype switching of vesicular glutamate transporters at parallel fibre-Purkinje cell synapses in developing mouse cerebellum. Eur J Neurosci 2003;17(12): 2563–2572. [PubMed: 12823463]

Miyazaki T, Hashimoto K, Shin HS, Kano M, Watanabe M. P/Q-type Ca2+ channel alpha1A regulates synaptic competition on developing cerebellar Purkinje cells. J Neurosci 2004;24(7):1734–1743. [PubMed: 14973254]

Nikonenko I, Jourdain P, Alberi S, Toni N, Muller D. Activity-induced changes of spine morphology. Hippocampus 2002;12:585–591. [PubMed: 12440574]

Nogradi A, Jonsson N, Walker R, Caddy K, Carter N, Kelly C. Carbonic anhydrase II and carbonic anhydrase-related protein in the cerebellar cortex of normal and lurcher mice. Brain Res Dev Brain Res 1997;98:91–101.

Okubo Y, Kakizawa S, Hirose K, Iino M. Visualization of IP(3) dynamics reveals a novel AMPA receptor-triggered IP(3) production pathway mediated by voltage-dependent Ca(2+) influx in Purkinje cells. Neuron 2001;32:113–122. [PubMed: 11604143]

Okubo Y, Kakizawa S, Hirose K, Iino M. Cross talk between metabotropic and ionotropic glutamate receptor-mediated signaling in parallel fiber-induced inositol 1,4,5-trisphosphate production in cerebellar Purkinje cells. J Neurosci 2004;24(43):9513–9520. [PubMed: 15509738]

Prange O, Murphy TH. Modular transport of postsynaptic density-95 clusters and association with stable spine precursors during early development of cortical neurons. J Neurosci 2001;21:9325–9333. [PubMed: 11717366]

Rhyu IJ, Abbott LC, Walker DB, Sotelo C. An ultrastructural study of granule cell/Purkinje cell synapses in tottering (tg/tg), leaner (tg(la)/tg(la)) and compound heterozygous tottering/leaner (tg/tg(la)) mice. Neuroscience 1999a;90:717–728. [PubMed: 10218773]

Rhyu IJ, Oda S, Uhm CS, Kim H, Suh YS, Abbott LC. Morphologic investigation of rolling mouse Nagoya (tg(rol)/tg(rol)) cerebellar Purkinje cells: an ataxic mutant, revisited. Neurosci Lett 1999b; 266:49–52. [PubMed: 10336181]

Sjoblom B, Elleby B, Wallgren K, Jonsson BH, Lindskog S. Two point mutations convert a catalytically inactive carbonic anhydrase-related protein (CARP) to an active enzyme. FEBS Lett 1996;398:322–325. [PubMed: 8977131]

Sotelo C, Hillman DE, Zamora AJ, Llinas R. Climbing fiber deafferentation: its action on Purkinje cell dendritic spines. Brain Res 1975;98:574–581. [PubMed: 1182538]

Takahashi KA, Linden DJ. Cannabinoid receptor modulation of synapses received by cerebellar Purkinje cells. J Neurophysiol 2000;83(3):1167–1180. [PubMed: 10712447]

Takayama C, Nakagawa S, Watanabe M, Mishina M, Inoue Y. Light- and electron-microscopic localization of the glutamate receptor channel delta 2 subunit in the mouse Purkinje cell. Neurosci Lett 1995;188:89–92. [PubMed: 7792064]

Takeuchi T, Miyazaki T, Watanabe M, Mori H, Sakimura K, Mishina M. Control of synaptic connection by glutamate receptor delta2 in the adult cerebellum. J Neurosci 2005;25(8):2146–2156. [PubMed: 15728855]

Westenbroek RE, Sakurai T, Elliott EM, Hell JW, Starr TV, Snutch TP, Catterall WA. Immunochemical identification and subcellular distribution of the alpha 1A subunits of brain calcium channels. J Neurosci 1995;15:6403–6418. [PubMed: 7472404]

Xu-Friedman MA, Harris KM, Regehr WG. Three-dimensional comparison of ultrastructural characteristics at depressing and facilitating synapses onto cerebellar Purkinje cells. J Neurosci 2001;21:6666–6672. [PubMed: 11517256]

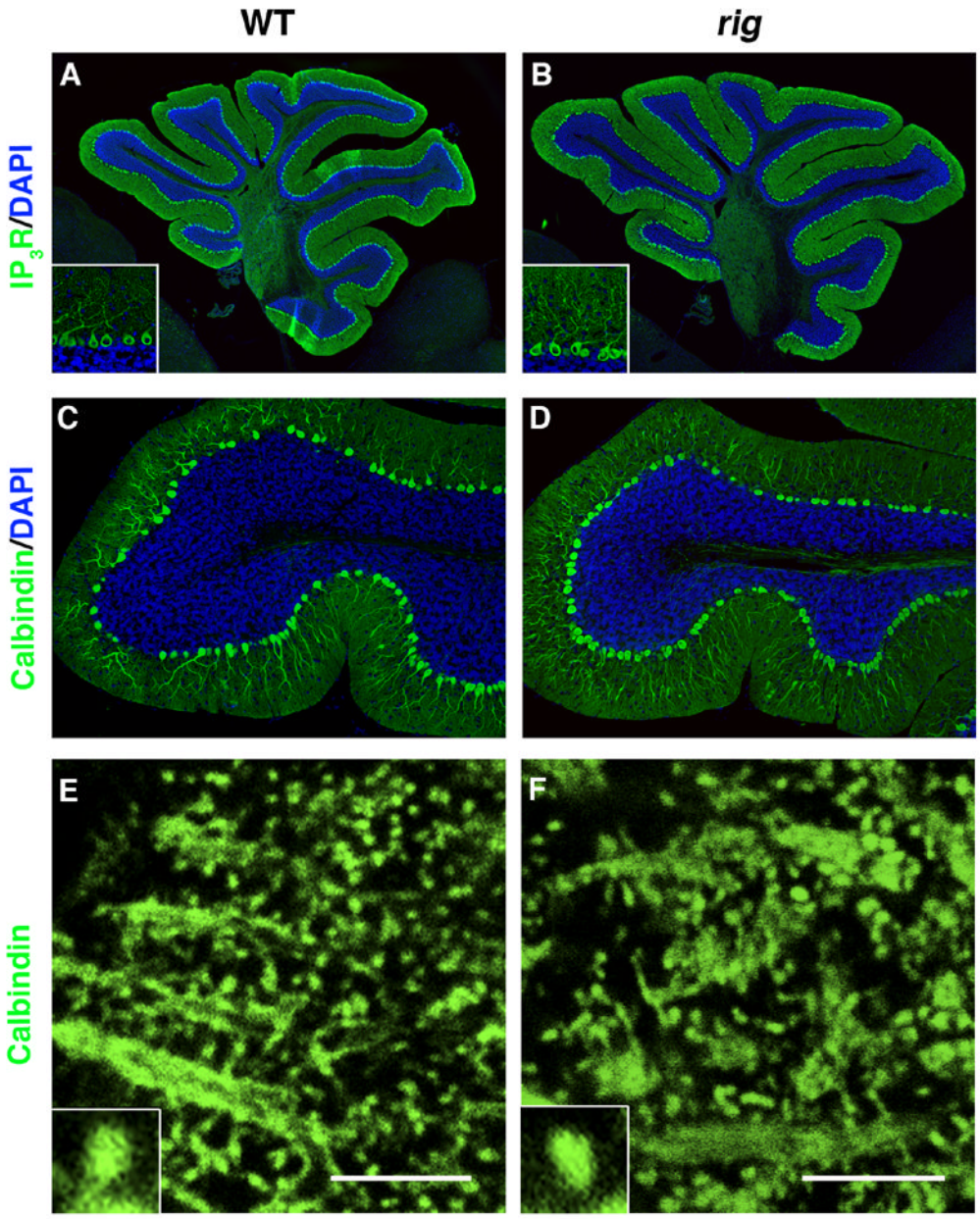

Fig. 1.

Immunohistochemical staining for Purkinje cell (PC) specific markers in the cerebellum of *rig* mice. (A, B) Wild-type (A) and *rig* (B) cerebellum stained with anti IP3 receptor (IP3R, green). Insets show higher magnification view of PCs. (C, D) The lobule IX of wild-type (C) and *rig* (D) cerebellum stained with anti Calbindin-D (green). Cell nuclei are counterstained with DAPI (blue) in A–D. (E, F) Calbindin-D staining showing the morphology of PC dendritic spines in wild-type (E) and *rig* (F) mice. Insets show higher magnification view of individual spines. Scale bars: 5 μm.

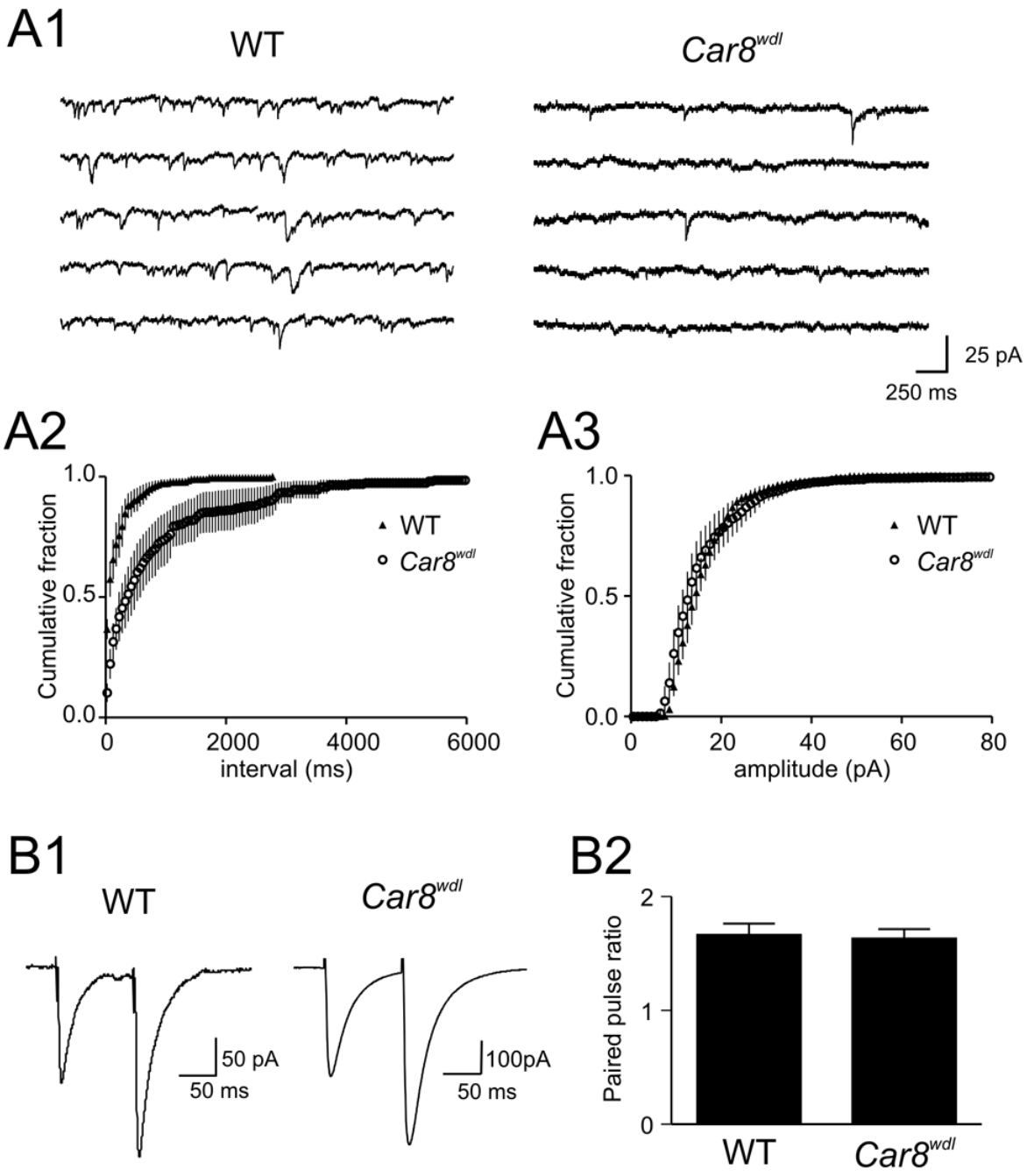

Fig. 2. Excitatory transmission is diminished in *Car8*^{wdl} mutants

(A1) Samples of mEPSCs recorded from Purkinje cells in wild-type or *Car8*^{wdl} mutant mice as indicated. (A2, A3) Cumulative plots of inter-event intervals (A2) and the amplitude (A3) of mEPSCs. The frequency of mEPSCs is significantly less in *Car8*^{wdl} mutants (A2) whereas there is no difference in the amplitude (A3). (B1) Representative recordings of EPSCs evoked by paired pulses. Both WT and *Car8*^{wdl} animals show paired pulse facilitation. (B2) Summary graph of paired pulse ratio, demonstrating no statistical difference between the two groups. Error bars in A2, A3 and B2 represent standard error.

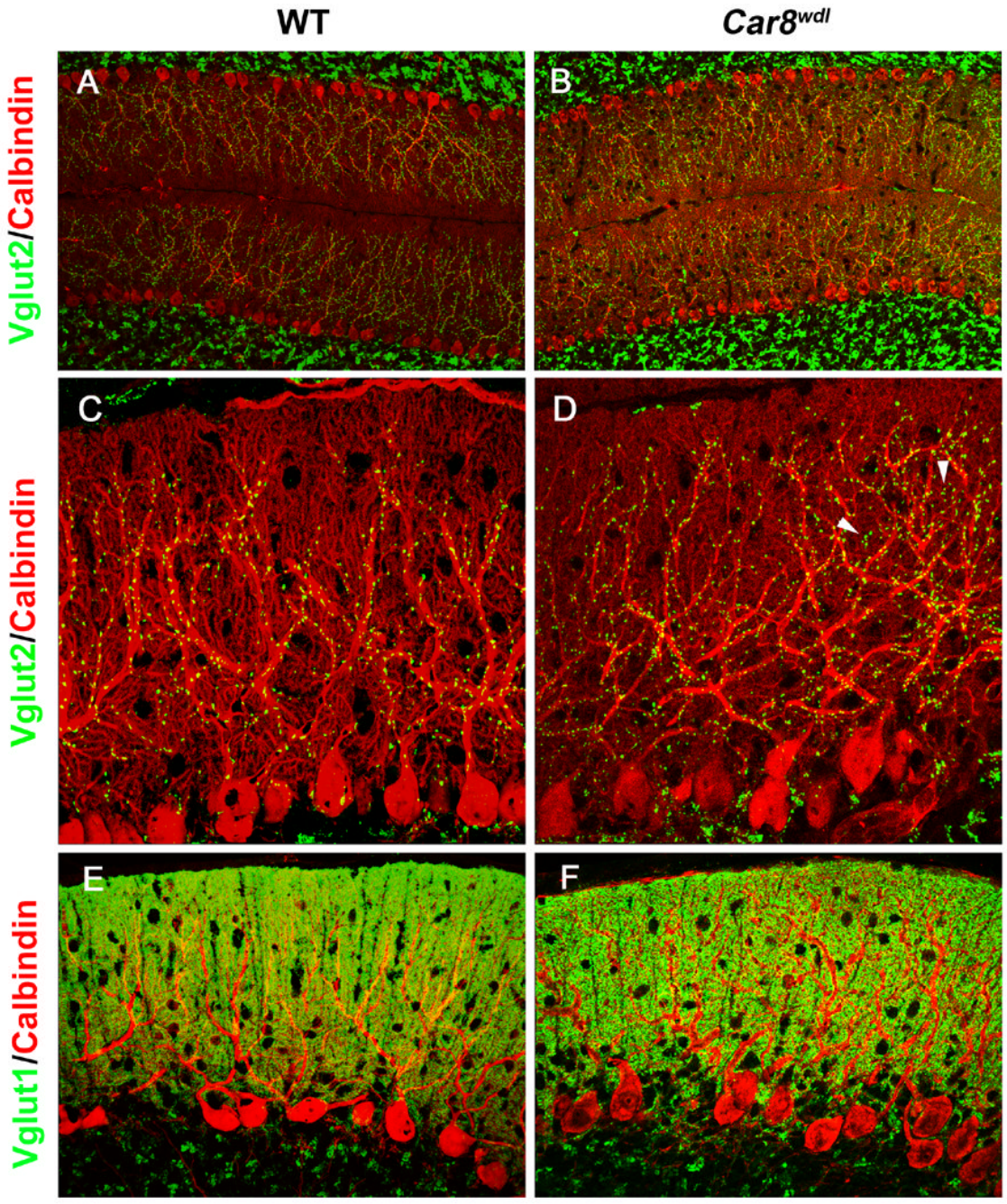

Fig. 3.

CF and PF labeling in the wild-type (A, C, E) and *Car8*^{wdl} (B, D, F) cerebellum. (A, B) Double immunofluorescence for VGLUT2 (green) and Calbindin (red). Note that the distribution of VGLUT2-labeled CF terminals is expanded distally in the molecular layer of *Car8*^{wdl} (B) compared to wild-type (A) mice. (C, D) Higher magnification view of VGLUT2 (green) and Calbindin (red) labeling. While VGLUT2 is mainly localized along the thick, proximal dendrites in wild-type mice (C), VGLUT2-labeled terminals are also associated with thinner, distal dendrites in *Car8*^{wdl} mice (D, arrowheads). Note an increase of VGLUT2-labeled puncta in the *Car8*^{wdl} molecular layer. (E, F) Double imunofluorescence for VGLUT1 (green) and

Calbindin (red). No overt difference in the distribution of VGLUT1-labeled PF terminals was detected between wild-type (E) and *Car8*^{wdl} (F) mice.

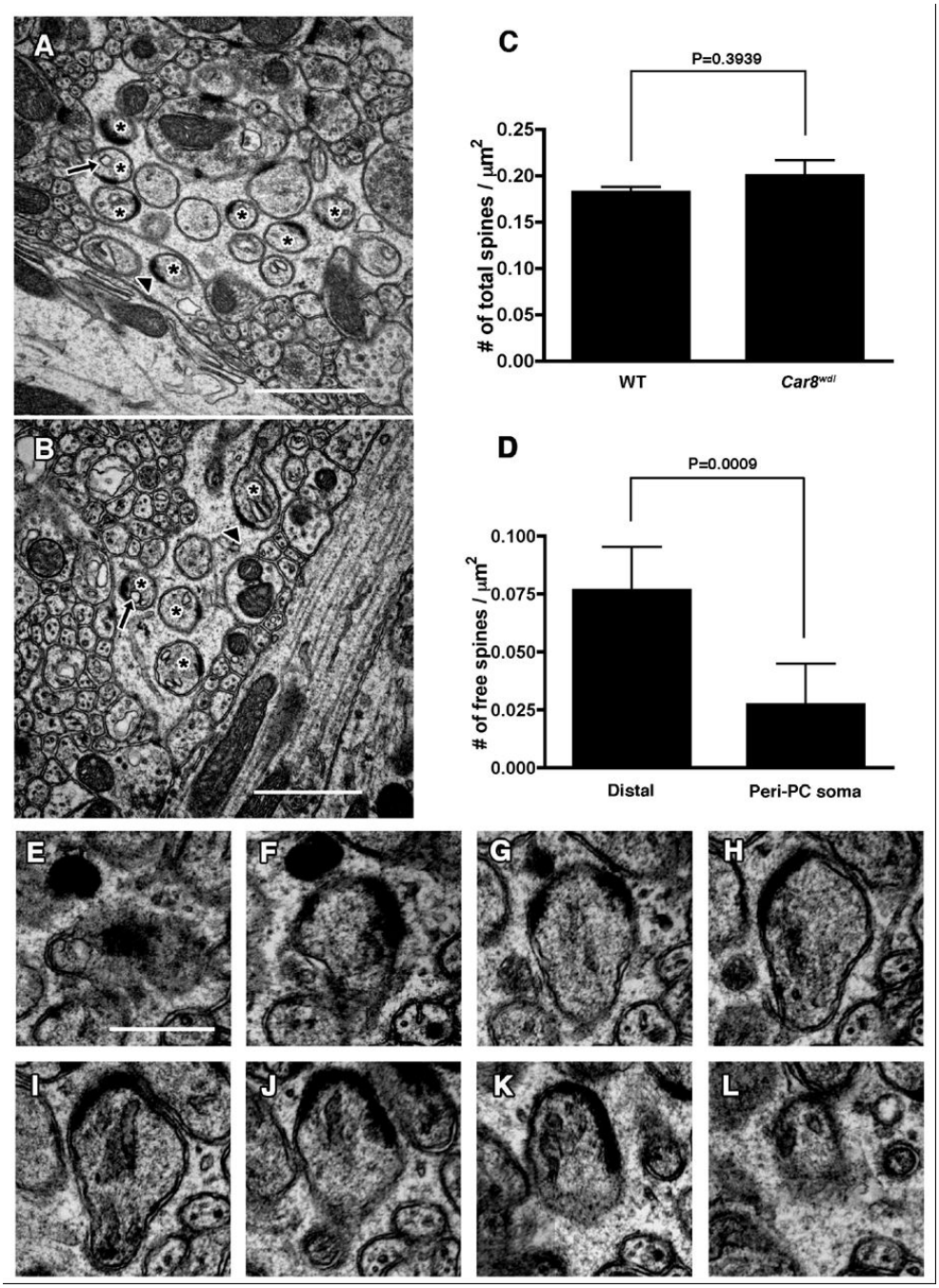

Fig. 4.

Electron micrographs of free dendritic spines in *Car8*^{wdl} cerebellum. (A–C) Numerous free spines are observed in clusters at various positions in the molecular layer of the cerebellum. Representative images are shown from distal (A) and proximal (B) dendritic field to the PC soma. Asterisks denote free spines. Note that free spines contain postsynaptic density (arrowheads) and endoplasmic reticulum (arrows). Scale bars: 1μm. (C) Number of PC dendritic spines per area in wild type (WT) and *Car8*^{wdl} mice. (D) Distribution of free spines in the molecular layer of *Car8*^{wdl} mice. Numbers of free spines per area in the region adjacent to the distal border of the molecular layer (distal) and the region adjacent to the PC soma (peri-PC soma) are shown. Error bars represent standard deviation. (E–L) Serial electron

micrographs of PC dendritic spine unattached to any nerve terminals (free spine) in *Car8*^{wdl} mice. Scale bar: 500nm.

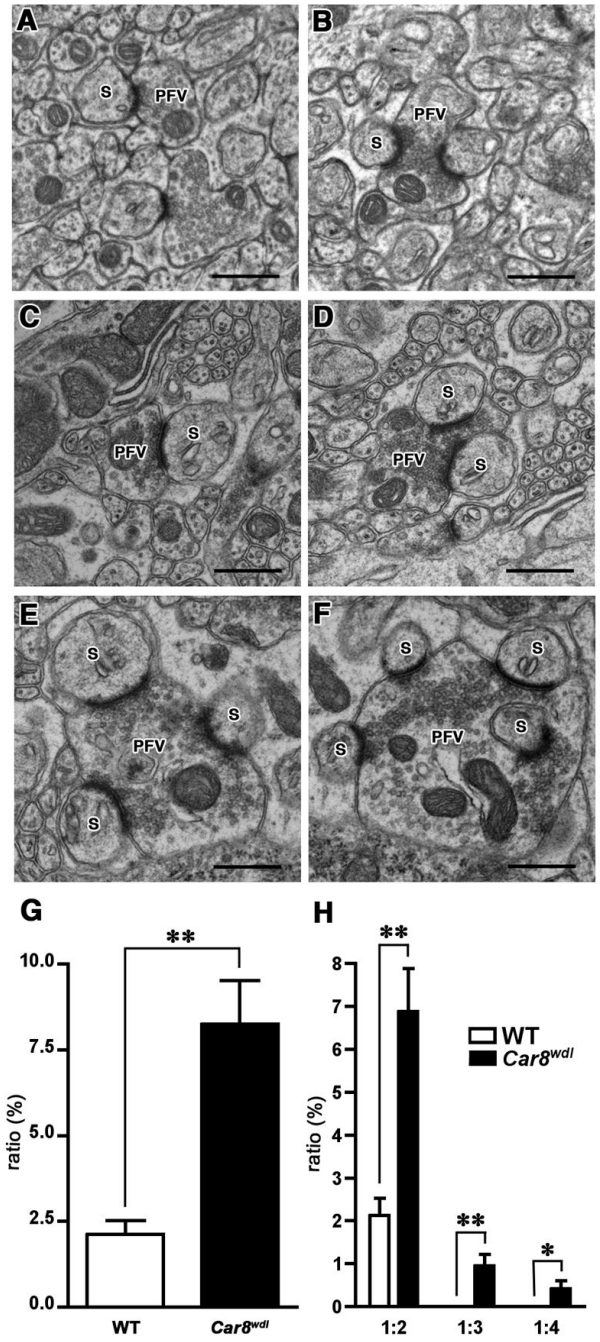

Fig. 5.

Electron microscopic analysis of excitatory synaptic contacts in wild-type and *Car8*^{wdl} cerebellum. In wild-type mice, parallel fiber varicosities interact with one (A) or two (B) dendritic spines of the PCs. In the *Car8*^{wdl} cerebellum, in addition to the varicosities interacting with one (C) or two (D) dendritic spines, those contacting more than two spines (E, F) are observed. S: dendritic spines, PFV: parallel fiber varicosity. Scale bar: 500 nm. As summarized in (G), the percentage of multiple synaptic varicosities (2–4 dendritic spines contacting 1 varicosity) against total synaptic interactions is significantly higher (**, $p<0.005$) in *Car8*^{wdl} mice. (H) shows the classification of multiple synaptic varicosities into 1:2 (presynapse vs

postsynapse), 1:3 and 1:4, and the percentage of multiple synaptic varicosities belonging to each class. ** and * denote statistical significance with $p<0.005$ and $p<0.05$, respectively.